https://doi.org/10.5194/egusphere-2026-3616
Preprint. Discussion started: 10 July 2026


# Simultaneous measurements of gas- and aerosol-phase water-soluble organic nitrogen in the winter urban atmosphere of Chengdu, China

Kaitao Chen[1], Zheng Li[1], Rui Li[1], Luyao Chen[1], Rongjie Li[1], Binyu Xiao[1], Shaojun Lv[1, ¶], Can Wu[1, 2], Rui Li[1, 2], Junke Zhang[3], Gehui Wang[1, 2, *]

[1]Key Laboratory of Geographic Information Science of the Ministry of Education, School of Geographic Sciences, East China Normal University, Shanghai 200241, China.
[2]Institute of Eco-Chongming, 20 Cuiniao Rd., Chongming, Shanghai 202150, China.
[3]Faculty of Geosciences and Environmental Engineering, Southwest Jiaotong University, Chengdu 611756, China.

[¶]Now at the State Key Laboratory of Advanced Environmental Technology, Guangzhou Institute of Geochemistry, Chinese Academy of Sciences, Guangzhou 510640, China.

[*] *Correspondence to*: Prof. Gehui Wang, Email：ghwang@geo.ecnu.edu.cn

https://doi.org/10.5194/egusphere-2026-3616
Preprint. Discussion started: 10 July 2026


**Abstract:** Partitioning gaseous water-soluble organic nitrogen (WSON) to the aerosol phase is a major formation pathway of atmospheric secondary organic aerosols (SOA). However, the factors influencing this WSON transfer process remain unclear. We conducted simultaneous wintertime measurements of WSON in both gas and aerosol phases at an urban site in Chengdu, located in the Sichuan Basin (SCB), China, to investigate the concentration, gas-particle partitioning processes, and driven factors of WSON. The average concentration of particulate WSON (2.3 ± 1.4 μgN $m^{-3}$) was about twice that of gaseous WSON (1.2 ± 0.9 μg N $m^{-3}$) and increased significantly as $PM_{2.5}$ increased. Amines (methylamine, MA; dimethylamine, DMA) were predominantly present in the gas phase but exhibited enhanced partitioning into the particle phase during the $PM_{2.5}$ polluted periods. The gas-particle partitioning coefficient ($F_{p(WSON)}$) showed a diurnal pattern with lower values during the day and higher values at night, which was enhanced by aerosol liquid water content (ALWC). Thermodynamic modeling using an S-curve analysis further revealed that ALWC was the key factor promoting the partitioning of WSON and amines into the particle phase, while the effects of pH and temperature were relatively weak. Furthermore, $NH_4NO_3$ was identified as the primary contributor to ALWC, suggesting that controlling $NO_x$ and $NH_3$ emissions is crucial for reducing ALWC and subsequent WSON formation.

https://doi.org/10.5194/egusphere-2026-3616
Preprint. Discussion started: 10 July 2026


## 1 Introduction

Organic nitrogen (ON) is a ubiquitous component of fine particulate matter ($PM_{2.5}$), accounting for 10%–50% of total nitrogen (TN) in global aerosols (Leung et al., 2024). Atmospheric nitrogen-containing organic compounds (NOCs) constitute a complex mixture, encompassing a wide range of compound classes, including urea, free and combined amino acids, amines, N-heterocyclic compounds, nitroaromatic hydrocarbons, nitrated polycyclic aromatic hydrocarbons, and organic nitrates (Jickells et al., 2013; Yu et al., 2024). These species partition between the gas and condensed phases depending on their volatility and water solubility. For example, low-molecular-weight amines and nitroaromatic compounds are semi-volatile and are distributed between the gas and particle phases (Liu et al., 2018; Chen et al., 2025). Monofunctional organic nitrates predominantly reside in the gas phase, whereas multifunctional organic nitrates exhibit substantially lower volatility and preferentially partition into the particle phase (Pleim and Ran, 2011).

Amines, as common water-soluble NOCs in the atmosphere, play a pivotal role in the formation and evolution of atmospheric aerosols. The sulfuric acid ($H_2SO_4$)-amine-$H_2O$ ternary nucleation theory has been widely recognized as a key mechanism for new particle formation (NPF), wherein amines markedly enhance nucleation rates compared to a $NH_3$ by stabilizing critical molecular clusters (Almeida et al., 2013; Schobesberger et al., 2013; Yao et al., 2018; Yu et al., 2025). Ambient observations have demonstrated more than a thousand-fold increase in particle formation rates in the presence of amines relative to ammonia (Kanawade and Jokinen, 2025). Moreover, even at sub-5 parts per trillion Volume (pptV) mixing ratios, amines can facilitate the physical and chemical transformation of aerosols, enhancing not only aerosol formation and growth rates but also hygroscopicity and the activation of cloud condensation nuclei (CCN) (Kanawade and Jokinen, 2025). Through acid-base reactions, amines readily form stable aminium salts (e.g., $H_2SO_4$-amines-$H_2O$) with inorganic acids, processes that can alter the physicochemical properties of pre-existing particles, including their hygroscopicity, thermostability, density, phase, and optical properties (Qiu and Zhang, 2013). Additionally, Maillard-like reactions between amines and carbonyl compounds in the aqueous phase contribute substantially to the formation of brown carbon (BrC), with organic amine precursors consistently yielding stronger light-absorbing capacities

https://doi.org/10.5194/egusphere-2026-3616
Preprint. Discussion started: 10 July 2026


compared to ammonium (Tang et al., 2022; Xiao et al., 2025). The gas-particle partitioning of amines is governed by multiple factors, including aerosol pH, relative humidity, and the composition of the condensed phase (Pankow, 2015). Notably, for several common amines, the tendency to partition into the particle phase is similar to or greater than that of $NH_3$, and such partitioning is strongly pH-dependent and maximized under acidic aerosol conditions (Ge et al., 2011). Despite the critical importance of amines in atmospheric chemistry and aerosol processes, research on their gas-particle partitioning behavior remains limited, hindering accurate assessment of their contribution to fine particulate matter formation and climate effects. Given the significant yet underexplored role of amines in aerosol formation, further investigation into their gas-particle partitioning mechanisms is urgently needed.

Water-soluble organic nitrogen (WSON) contributes significantly to the formation of SOA. Typically, WSON accounts for 8–30% of the water-soluble total nitrogen (WSTN) mass in atmospheric aerosols, as well as in snow and rain (Mochizuki et al., 2016; Yu et al., 2020; Murray et al., 2022). In regions influenced by fossil fuel and biomass combustion, the WSON/WSTN ratio can reach 60% (Nehir and Koçak, 2018). However, reports on gaseous WSON remain scarce, with most studies focusing on the particle phase, leading to a limited understanding of the atmospheric nitrogen cycle and atmospheric brown carbon. Research on the gas-particle partitioning behavior of WSON is even more lacking. Therefore, this study conducted an intensive winter observation campaign in the Sichuan Basin (SCB) from December 2024 to January 2025. Our work aims to elucidate the pollution characteristics of WSON and amines, and the driving factors governing their gas-particle partitioning behavior in the atmosphere.

## 2 Materials and methods

### 2.1 Observation site description.

Winter sampling was conducted in Chengdu, located in the SCB, from December 14, 2024, to January 9, 2025. The observation site was situated on the roof of the Civil Engineering Building at Southwest Jiaotong University's Jiuli Campus (30.7°N, 105.05°E) (Fig. S1), at a height of 25 meters above ground level. It was located in the central area of Chengdu, near the North Second Ring Road, surrounded by residential areas, shopping malls, gas stations, and restaurants, During the sampling period,

https://doi.org/10.5194/egusphere-2026-3616
Preprint. Discussion started: 10 July 2026


meteorological conditions in Chengdu were stagnant with low wind speeds and high relative humidity (RH) (Table 1).

### 2.2 Measurements of the gas- and aerosol-phase species.

Continuous measurements of inorganic ions, WSON, MA, and DMA in the gas and aerosol phases were conducted at the campus site. Online samples of the aforementioned compounds were collected via the In-situ Gas and Aerosol Compositions monitor (IGAC, model 63GA, Fortelice International Co., Ltd., Taiwan, China) coupled with an ICS–5000+ ion chromatograph (Thermo Scientific，USA) and a TOC/TN analyzer (model TOC/TN–L CPH, Shimadzu, Inc., Japan) for simultaneous measurements of online samples. WSON was measured with a time interval of 3 hours, while other species were measured hourly. In this study, the equation for calculating WSON concentration is as follows:

$$WSON_{g,p}=WSTN_{g,p} - WSIN_{g,p} \quad (1)$$

where, g and p represent the gas phase and particle phase, respectively; WSTN represents total water-soluble nitrogen measured by TOC/TN analyzer; WSIN represents the total water-soluble inorganic nitrogen measured by IGAC–IC. The unit is μg $m^{-3}$. Due to the differing forms in which inorganic nitrogen exists in the gas phase and particulate phase, the calculation methods will vary accordingly, as follows:

$$WSIN_g=\left(\frac{[NH_3]}{17}+\frac{[HNO_3]}{63}+\frac{[HNO_2]}{47}\right)\times 14 \quad (2)$$

$$WSIN_p=\left(\frac{[NH_4^+]}{18}+\frac{[NO_3^-]}{62}+\frac{[NO_2^-]}{46}\right)\times 14 \quad (3)$$

Five anions ($SO_4^{2-}$, $NO_3^-$, $NO_2^-$, $Cl^-$, $F^-$), five cations ($NH_4^+$, $Na^+$, $K^+$, $Mg^{2+}$, $Ca^{2+}$), and two amines (MA and DMA) were measured in this study. $PM_{2.5}$ and meteorological parameters (including temperature and RH) were measured by the E–BAM continuous environmental $PM_{2.5}$ monitor (Met One Instruments, United States) and an automatic weather station (MILOS520, Vaisala, Inc., Finland), respectively. In this study, pollution periods (PP) were defined as days with a daily $PM_{2.5}$ > 75 μg $m^{-3}$, clean periods (CP) as $PM_{2.5}$ < 35 μg $m^{-3}$, and transition periods (TP) as $PM_{2.5}$ between 35 and 75 μg $m^{-3}$. The organic carbon (OC) and elemental carbon (EC) of the $PM_{2.5}$ filter samples were analyzed by DRI Model 2015 Carbon

https://doi.org/10.5194/egusphere-2026-3616
Preprint. Discussion started: 10 July 2026


Analyzer (Atmoslytic, Inc., Calabasas, USA) with IMPROVE_A protocol (Chow et al., 2012; Li et al., 2025).

To minimize background interference and systematic errors in the instrument, a HEPA filter was installed at the IGAC sampling port. Measurement results indicated that the background levels in the tube system were comparable to the blank concentration of deionized water. The background concentrations of WSOC and WSTN in the tubes were 0.049 ± 0.030 mg $L^{-1}$ and 0.007 ± 0.002 mg $L^{-1}$, respectively, significantly lower than the sample concentrations. Additionally, the collection efficiency of IGAC system for both gas and particle phase species is $>$ 73% (Lv et al., 2022a; Lv et al., 2022b), and the data during the observation period were corrected accordingly. For detailed information on instrument applications and method accuracy tests, please refer to the Support Information Text S1.

### 2.3 Calculations on ALWC and acidity of $PM_{2.5}$.

The ALWC and acidity (pH) of $PM_{2.5}$ were estimated using the thermodynamic ISORROPIA-II model based on hourly data of aerosol chemical composition (including $Na^+$, $NH_4^+$, $K^+$, $Ca^{2+}$, $Mg^{2+}$, $SO_4^{2-}$, $NO_3^-$, and $Cl^-$), gaseous $NH_3$ concentration, and meteorological parameters (T; RH) (Fountoukis and Nenes, 2007). The forward metastable mode was employed for the estimation due to its lower sensitivity to measurement errors compared to the reverse mode (Hennigan et al., 2015). Data corresponding to RH greater than 95% were excluded on the basis that such conditions are associated with increased uncertainty in the model estimation of both ALWC and pH (Guo et al., 2015). The contribution of organic compounds to ALWC ($ALWC_{org}$) was determined using the mass concentration of organic matter (OM) (Lv et al., 2022a; Lv et al., 2022b), as described in detail in the Supporting Information Text S2.

### 2.4 S-Curve analysis of amines.

To further elucidate the effects of pH and ALWC on the gas-particle phase distribution of organic amines, this study assumes that the gas and particle phases of amines are in thermodynamic equilibrium. $\varepsilon(CH_3NH_3^+)$ and $\varepsilon((CH_3)_2NH_2^+)$, the theoretical values of the gas-particle phase distribution coefficients, are calculated using a thermodynamic model and analyzed via S-curve analysis with aerosol pH.

https://doi.org/10.5194/egusphere-2026-3616
Preprint. Discussion started: 10 July 2026


The calculation equations are as follows:

$$\varepsilon(CH_3NH_3^+)=\frac{\left(\frac{\gamma_{H^+}}{\gamma_{CH_3NH_3^+}}10^{-pH}+\frac{K_a}{\gamma_{CH_3NH_2}}\right)\frac{H_{CH_3NH_2}}{K_a}W_iRT\times0.987\times10^{-14}}{1+\left(\frac{\gamma_{H^+}}{\gamma_{CH_3NH_3^+}}10^{-pH}+\frac{K_a}{\gamma_{CH_3NH_2}}\right)\frac{H_{CH_3NH_2}}{K_a}W_iRT\times0.987\times10^{-14}} \quad (4)$$

$$\varepsilon((CH_3)_2NH_2^+)=\frac{\left(\frac{\gamma_{H^+}}{\gamma_{(CH_3)_2NH_2^+}}10^{-pH}+\frac{K_a}{\gamma_{(CH_3)_2NH}}\right)\frac{H_{(CH_3)_2NH}}{K_a}W_iRT\times0.987\times10^{-14}}{1+\left(\frac{\gamma_{H^+}}{\gamma_{(CH_3)_2NH_2^+}}10^{-pH}+\frac{K_a}{\gamma_{(CH_3)_2NH}}\right)\frac{H_{(CH_3)_2NH}}{K_a}W_iRT\times0.987\times10^{-14}} \quad (5)$$

where, $H_i$ is the Henry's law constant for organic amine i at 298.15 K, $K_a$ is acid dissociation constant at 298.15 K, $\gamma_i$ represents the activity coefficient, which can be calculated using the E-AIM model; $W_i$ is the ALWC of the particles; R is the gas constant, and T is the temperature. Detailed derivations of Equations (4) and (5) are provided in the Support Information Text S3.

## 3 Results and discussion

### 3.1 Chemical characteristics of $PM_{2.5}$ pollution during the campaign.

The temporal variations of meteorological parameters, major atmospheric pollutants during the whole campaign are shown in Fig. 1 and Table 1, respectively. During the campaign, the average $PM_{2.5}$ concentration in Chengdu was 76 ± 38 μg $m^{-3}$ (Table 1), with 14 pollution days accounting for 51.9% of the total sampling days. The average $PM_{2.5}$ concentration during PP was 100 ± 33 μg $m^{-3}$, with the highest pollution level reaching 199 μg $m^{-3}$. Concurrently, $NO_3^-$ concentrations (Table S1) and contributions (Table S1) began to exceed those of $SO_4^{2-}$ and exhibited an overall increasing trend, indicating that $NO_3^-$ has become the dominant inorganic salt in $PM_{2.5}$. In contrast, $SO_4^{2-}$ remained relatively stable and was significantly lower in 2024 compared to previous years (Table S1). $NH_4^+$ has remained relatively stable since its decline began in 2016, as has $Cl^-$. In this study, $SO_4^{2-}$, $NO_3^-$, and $NH_4^+$ accounted for 7.2 ± 3.1%, 22.8 ± 6.6%, and 11.5 ± 4.6% of the $PM_{2.5}$ mass, respectively (Fig. 1b). Additionally, the observed concentration of organic matter (OM) in Chengdu was 21.1 ± 9.6 μg $m^{-3}$ (Table 1), contributing 27.3 ± 7.4% to the total $PM_{2.5}$ mass. As shown in Table S1, previously reported values in the SCB also exceeded 25%. These results clearly indicate that $NO_3^-$ and OM are the major

https://doi.org/10.5194/egusphere-2026-3616
Preprint. Discussion started: 10 July 2026


components of $PM_{2.5}$ in the SCB, accounting for over 50% of the total $PM_{2.5}$ mass.

The temporal variation of $WSON_p$ (Fig. 1c) exhibited the same trend as $PM_{2.5}$ (Fig. 1b), with a significant positive correlation between $WSON_p$ and $PM_{2.5}$ ($R = 0.78$, $p < 0.05$, Fig. Table S1). $WSON_p$ contributed to 0.5 – 12.4% of the $PM_{2.5}$ mass, with the average value was 3% (Fig. S3a–d). The concentration of $WSON_p$ (2.7 ± 1.6 μg $m^{-3}$) was more than twice that of $WSON_g$ (1.2 ± 0.9 μg $m^{-3}$) (Fig. 1c and Table 1), indicating that WSON in the SCB mainly exists in the particle phase, as observed at Mt. Fuji in Japan (Matsumoto et al., 2020). WSON contributed 9.3% and 14.7% to the total nitrogen (TN) in the gas phase and particulate phase, respectively. In Chengdu, the WSON/WSOC ratios for the gas and particle phases were 0.05 and 0.15 (Fig. S3e–l), respectively. Notably, the $WSON/WSOC_p$ ratio increases as pollution worsens (Fig. S3i–l), indicating that more NOCs are formed during the accumulation of OM. Our study shows that the wintertime $WSON_p$ concentration of $PM_{2.5}$ in Chengdu (2.3 ± 1.4 μgN $m^{-3}$) was slightly higher than those in central Chinese cities such as Nanjing (1.7 ± 0.6 μgN $m^{-3}$) (Guan et al., 2022) and Shanghai (1.9 ± 1.8 μgN $m^{-3}$) (Lv et al., 2022a), as well as in the northern city of Wuhai (1.7 ± 1.1 μgN $m^{-3}$) (Xie et al., 2025), but substantially higher than those in southern coastal cities such as Guangzhou (0.48 – 0.53 μgN $m^{-3}$) (Yu et al., 2017) and Hong Kong (0.6 ± 0.6 μgN $m^{-3}$) (Leung et al., 2024). This indicates that the wintertime NOCs of $PM_{2.5}$ in Chengdu are notably prominent, likely due to its unique basin topography, which allows local emissions (e.g., biomass burning (Yu et al., 2017; Xie et al., 2025), cooking fumes (Özel et al., 2010; Ditto et al., 2022), vehicle exhaust (Yu et al., 2017; Xie et al., 2025)) and secondary formation (Liu et al., 2023; Yu et al., 2017; Xie et al., 2025) to continuously accumulate near the surface, resulting in concentrations that exceed those in other cities.

### 3.2 Gas-to-aerosol phase partitioning of WSON

Table S2 and Fig. S4 illustrate the diurnal variations in gas- and particle-phase concentrations of WSON and its gas-particle partitioning coefficient ($F_{WSON}$) across different pollution periods (clean, transition, and pollution). $WSON_{g,p}$ concentrations were low during the CP and showed no significant diurnal variation ($p > 0.05$). $WSON_{g,p}$ began to gradually increase within the TP. During the PP, $WSON_{g,p}$ increased significantly during the day ($p < 0.01$), exhibiting distinct photochemical

https://doi.org/10.5194/egusphere-2026-3616
Preprint. Discussion started: 10 July 2026


characteristics. Wang et al. (2024) reported that photochemical reactions were a major cause of winter haze formation in the SCB, and the polluted period showed a much higher degree of photochemical aging compared to the non-pollution period. Similar $WSON_p$ formation due to photochemical oxidation during winter has also been observed in Hong Kong (Leung et al., 2024). Based on previous studies, there are three primary pathways for the secondary formation of $WSON_{g,p}$ (Fig. S5): (1) aqueous-phase reaction of $NH_3/NH_4^+$ with biogenic volatile organic compounds (BVOCs) to form water-soluble NOCs including imidazoles and other species (Stangl and Johnston, 2017; Xiao et al., 2025); the significant positive correlation between $WSON_p$ and $NH_3/NH_4^+$ in Chengdu ($R > 0.5$, $p < 0.05$) (Fig. S6) confirms this pathway. Additionally, the "salting-in" effect induced by sulfate and nitrate promotes the partitioning of polar organics (e.g., glyoxal) into the aerosol aqueous phase, enhancing NOCs formation (Sareen et al., 2017; Gen et al., 2018), which is consistent with the significant correlations between $WSON_p$ and both $SO_4^{2-}$ and $NO_3^-$ in Chengdu ($R > 0.6$, $p < 0.05$) (Fig. S6); (2) reaction of $NO_x$ with BVOCs to form gaseous NOCs, which subsequently enter the particulate phase via gas-to-particle conversion (Xie et al., 2025; Nursanto et al., 2026; Xu et al., 2026; Zhang et al., 2026); (3) photochemical reactions of BTEX (benzene, toluene, ethylbenzene, xylene) with OH and $NO_3$ radicals to form gaseous nitrophenols, which then partition into the particulate phase, while BTEX can also be directly absorbed into the particulate phase and undergo liquid-phase reactions to form $WSON_p$ (Vione et al., 2004; Yuan et al., 2016; Wang et al., 2019; Chen et al., 2025).

As shown in Fig. S4 and Table S2, $F_{WSON}$ remained approximately 0.60 during the CP with no significant diurnal variation ($p > 0.05$). Starting from the TP, it exhibited a pronounced pattern of lower values during the day ($0.60 \pm 0.15$) and higher values at night ($0.71 \pm 0.12$) ($p < 0.01$), which persisted into the PP (day: $0.69 \pm 0.13$, night: $0.76 \pm 0.12$, $p < 0.01$). In both periods, the minimum value occurred around noon. This partitioning characteristic may suggest that photochemical oxidation reactions rapidly generate $WSON_g$ during the daytime (Rollins et al., 2010), followed by its partitioning into the particulate phase. Figure 2 shows that $F_p$ exhibited no significant correlations with T, RH or pH ($R < 0.3$), indicating that it is weakly regulated by these factors. Therefore, the decrease in $F_{WSON}$ during the daytime may be attributed to the increase of $WSON_g$ exceeding that of $WSON_p$ (Fig. S4). At nighttime, the combination of depleted gas-phase precursors and

https://doi.org/10.5194/egusphere-2026-3616
Preprint. Discussion started: 10 July 2026


aqueous-phase/heterogeneous reactions promoted by ALWC leads to relative enrichment of $WSON_p$ (Xu et al., 2020; Leung et al., 2024) and an increased $F_{WSON}$ value. Meanwhile, ALWC showed weak correlations with both $WSON_p$ and $F_p$ ($R = 0.31$ (Fig. S6) and $R = 0.32$ (Fig. 2), respectively; $p < 0.05$), which is inconsistent with previous studies reporting stronger correlations ($R > 0.5$) (Xu et al., 2020; Leung et al., 2024). This discrepancy may stem from the high OM loading in Chengdu's atmosphere (Table 1). The ratio of OM to inorganic ions in Chengdu's atmosphere is as high as 0.70, suggesting that organic gases can form a hydrophobic outer layer on the surface of inorganic salt nuclei, creating a core-shell structure that weakens the transfer of gases to the particle phase (Silvern et al., 2017), and ultimately leading to the weak correlations of ALWC with $WSON_p$ and $F_p$.

To further investigate the influence of ALWC on the partitioning of WSON in China, we conducted a statistical analysis of the relationship between the spatial distribution of the ratio of ALWC to $PM_{2.5}$ ($f_{ALWC}$) and $F_{WSON}$ across the country (Fig. 3a). A significant linear correlation was observed between $f_{ALWC}$ and $F_{WSON}$ ($R = 0.78$, $p < 0.05$), indicating that higher ALWC levels promote the partitioning of $WSON_g$ into the particle phase. As illustrated in Fig. 3b, ALWC increased with increasing SNA (sulfate, nitrate, ammonium) concentrations during the observation period, particularly under conditions of high RH. Calculations using the ISORROPIA-II thermodynamic model indicate that $NH_4NO_3$ contributed approximately 61.3% to ALWC, followed by $(NH_4)_2SO_4$ (14.4%) and OM (7.7%) during the whole campaign in the SCB (Fig. 3c). Figure 3d demonstrates that ALWC increased with the ratio of $NH_4NO_3$ to $PM_{2.5}$ at a given RH, suggesting that ALWC in the SCB during winter is primarily driven by $NH_4NO_3$. Therefore, controlling emissions of $NH_4NO_3$ precursors ($NO_x$ and $NH_3$) is crucial for both ALWC and WSON.

### 3.3 Gas-to-aerosol phase partitioning of amines

Numerous studies have demonstrated that amines play an important role in new particle formation and growth, as observed in both field measurements (Yu et al., 2012; Tao et al., 2016; Yao et al., 2018) and laboratory simulations (Almeida et al., 2013; Kürten et al., 2014; Lehtipalo et al., 2016). In the SCB, amines contribute significantly to $WSON_{g,p}$. Specifically, amines-N (MA-N and DMA-N) account for 48.7% and 10.5% of WSON in the gas and particle phases, respectively (Fig. 4).

https://doi.org/10.5194/egusphere-2026-3616
Preprint. Discussion started: 10 July 2026


During the winter haze periods in the CD, the total concentration of amines increased substantially, and the gas-particle partitioning coefficient (F) nearly doubled (Table 1), indicating enhanced gas-to-particle conversion. The high volatility of amines can easily lead to their transfer into the gas phase. As shown in Fig. 1d and Table 1, the gas-phase concentrations of methylamine ($MA_g$) and dimethylamine ($DMA_g$) (1.23 ± 0.37 μg $m^{-3}$ and 0.41 ± 0.03 μg $m^{-3}$, respectively) were 3-5 times higher than their particle-phase concentrations (0.45 ± 0.24 μg $m^{-3}$ and 0.09 ± 0.05 μg $m^{-3}$, respectively). This trend was consistent with observations reported from the Nanling Mountains in Guangzhou, China ($MA_g$: 60.6 ± 35.0 ng $m^{-3}$, $MA_p$: 8.8 ± 7.8 ng $m^{-3}$; $DMA_g$: 71.3 ± 54.5 ng $m^{-3}$, $DMA_p$: 2.4 ± 3.2 ng $m^{-3}$) (Liu et al., 2018), suggesting that amines predominantly exist in the gas phase in the atmosphere. Furthermore, the observed amine concentrations were much higher than those reported in other regions (Liu et al., 2018; Yang et al., 2022; Zhu et al., 2022; Yang et al., 2023; Brean et al., 2025). Studies show that vehicle emissions elevate roadside $C_1$–$C_2$ amine concentrations by more than a factor of four relative to background levels (Brean et al., 2025), with a contribution exceeding 70% (Yang et al., 2022; Zhu et al., 2022). As shown in Fig. S7, amines in Chengdu exhibited significant correlations with the vehicular tracers $NO_2$ and CO ($r = 0.4$ and 0.5, respectively, $p < 0.05$), indicating that vehicle exhaust contributes to amine emissions to some extent.

Except primary emissions, secondary formation also was a major source of amines (Yang et al., 2023). In Chengdu, particulate amines exhibited strong correlation with SNA ($r > 0.7$, $p < 0.05$; Fig. S6), indicating that secondary formation driven by acid–base neutralization is also an important source. According to the Reactions (6 – 7) (Ge et al., 2011), gaseous amines synergistically neutralize $H_2SO_4$/$HNO_3$ together with $NH_3$ to generate particulate amine salts (Almeida et al., 2013; Glasoe et al., 2015; Liu et al., 2018). The humid and stagnant meteorological conditions in the SCB (Table 1) provide an ideal environment for the above transformations, promoting efficient enrichment of amines in the particle phase and making them a significant component of water-soluble ions in $PM_{2.5}$.

$$R_nNH_{3-n}(g) \rightleftharpoons R_nNH_{3-n}(aq) \quad (6)$$

$$R_nNH_{3-n}(aq) + H_2O(l) \rightleftharpoons R_nNH_{4-n}^{+}(aq) + OH^{-}(aq) \quad (7)$$

$$R_nNH_{4-n}^{+}(aq) + NO_3^{-}/SO_4^{2-}(aq) \rightleftharpoons R_nNH_{4-n}NO_3\ (s)/(R_nNH_{4-n})_2SO_4\ (s) \quad (8)$$

$$R_nNH_{3-n}(g) + HNO_3\ (g)/H_2SO_4\ (g) \rightleftharpoons R_nNH_{4-n}NO_3\ (s)/(R_nNH_{4-n})_2SO_4\ (s) \quad (9)$$

https://doi.org/10.5194/egusphere-2026-3616
Preprint. Discussion started: 10 July 2026


Figure 5a and 5b present the theoretical values of the gas-particle partitioning coefficients for MA and DMA ($\varepsilon(CH_3NH_3^+)$ and $\varepsilon((CH_3)_2NH_2^+)$, respectively) calculated using a thermodynamic model and plotted against aerosol pH in an S-curve analysis. The observed partitioning coefficients for amines in the SCB fell within the range predicted by theoretical calculations; however, they did not exhibit the anticipated decrease with increasing pH. Theoretically, the partitioning of amines is co-regulated by pH, ALWC, and T. Under acidic conditions with low pH, amines are protonated to form ionic species, with ε approaching 100%, favoring their partitioning into the aerosol phase. As pH increases, deprotonation occurs, forming volatile free bases, with ε approaching 0, leading to their transfer to the gas phase. However, given the acidity of atmospheric aqueous phases (pH 0–5), amines exist almost entirely in their protonated form ($R\text{-}NH_3^+$), rendering them largely insensitive to pH variations (Tilgner et al., 2021). Generally, lower temperatures enhance the effective solubility of trace gases. However, Tilgner et al. (2021) explicitly noted that aqueous-phase partitioning coefficients are higher in clouds (typically around 285 K) compared to near-surface conditions during hot summers, and higher in winter compared to summer. This indicates that the influence of T on partitioning coefficients is manifested in vertical altitude gradients and seasonal variations. Within a single season, its impact is less pronounced compared to that of ALWC (Tilgner et al., 2021). In this study, the partitioning coefficients of amines showed no significant correlation with T but exhibited a significant positive correlation with ALWC (Fig. 2). Consequently, variations in pH and T exert minimal influence on amine partitioning, with ALWC emerging as the dominant limiting factor. ALWC significantly promotes the enrichment of amines in the particle phase ($p < 0.05$, Fig. S6) and enhances their partitioning ($p < 0.05$, Fig. 2).

According to the Pankow (1994), aerosol mass loading may also be a factor affecting the gas-particle partitioning of organic compounds (Pankow, 1994; Lutz et al., 2019; Li et al., 2025). This relationship is typically described using Raoult's law, with the calculation equation as follows (Pankow, 1994):

$$K_i = \frac{[i]_{particle}}{[i]_{gas}\,\mathrm{TSP}} \tag{10}$$

where $K_i$ is the partitioning constant of compound $i$, $[i]_{particle}$ and $[i]_{gas}$ represent

https://doi.org/10.5194/egusphere-2026-3616
Preprint. Discussion started: 10 July 2026


the concentrations of compound *i* in the particle and gas phases, respectively, and TSP is the concentration of total suspended particulate material ($PM_{2.5}$ mass concentrations are used in this study). Figure S8 shows the relationship between the $[i]_{particle}/[i]_{gas}$ ratios of MA and DMA and $PM_{2.5}$ mass concentrations during the clean, transition, and pollution periods, respectively. For MA, the correlations between its $[i]_{particle}/[i]_{gas}$ ratio and $PM_{2.5}$ were weak across all the three periods, with $R < 0.5$ and $p < 0.01$. The $[i]_{particle}/[i]_{gas}$ ratio of DMA during the clean period showed a correlation with $PM_{2.5}$ ($R = 0.56$, $p < 0.01$); however, according to the application criteria for the $K_i$ value proposed by Lutz et al. (2019), an $R^2$ greater than 0.7 is required for accurate $K_i$ determination and meaningful interpretation, indicating that the results did not fall within the applicability range in this study. During the transition and pollution periods, the $[i]_{particle}/[i]_{gas}$ ratio of DMA also showed no significant correlation with $PM_{2.5}$ ($R < 0.4$, $p < 0.01$), suggesting that aerosol mass loading did not exert a significant influence on amines uptake during the sampling period.

## 4 Summary and implications

Atmospheric WSON accounts for approximately one-quarter to one-third of TN in global wet deposition. Its chemical composition is highly complex, and its qualitative and quantitative characterization remains limited to date (Yu et al., 2020). The environmental behavior of WSON in the atmosphere (e.g., residence time, transformation pathways, and deposition mechanisms) is influenced by its gas-particle partitioning coefficient ($F_{WSON}$). However, relevant studies are still lacking, and most existing research has only measured particle-phase WSON. The SCB, characterized by its unique topography and frequent stagnant, high-humidity meteorological conditions in winter, is one of the regions most severely affected by haze in China. Secondary inorganic ions account for 40%–60% of $PM_{2.5}$ mass (Zhang et al., 2024a; Zhang et al., 2024b), and the gas-particle partitioning of nitrogen-containing organic compounds is strongly affected by the high-humidity environment.

In this study, IGAC was employed to simultaneously measure, for the first time in the Sichuan Basin, the concentration levels, chemical composition, and partitioning characteristics of wintertime gas- and particle-phase WSON. The evolution of WSON gas-particle partitioning across different pollution stages and its key driving factors

https://doi.org/10.5194/egusphere-2026-3616
Preprint. Discussion started: 10 July 2026


were systematically elucidated. This study found that in high-humidity environments, ALWC plays a much stronger role in promoting the partitioning of WSON and amines into the particle phase than pH or T. During the PP, the particle-phase partitioning coefficients of amines increased significantly. Owing to their stronger basicity compared to $NH_3$, amines can more effectively undergo acid-base reactions with acidic molecules such as sulfuric acid, forming more stable sulfuric acid–amine–water clusters, thereby substantially enhancing new particle formation rates (Almeida et al., 2013; Schobesberger et al., 2013; Yao et al., 2018). This indicates that amines are important precursors for SOA formation during heavy pollution episodes. Thermodynamic model (ISORROPIA-II) and S-curve analysis revealed that ALWC is the dominant factor controlling the partitioning of NOCs. This finding suggests that in high-humidity polluted regions, aqueous-phase chemical processes contribute significantly to nitrogen-containing organic aerosol formation. Studies by Yu et al. (2017), Xu et al. (2020) and Leung et al. (2024) have similarly demonstrated that ALWC significantly promotes the secondary formation of particle-phase WSON. $NH_4NO_3$ contributes approximately 61% of ALWC, making it the largest contributor. Therefore, for SCB, synergistic control of $NO_X$ and $NH_3$ emissions can not only directly reduce nitrate in $PM_{2.5}$ but also indirectly inhibit the particle-phase enrichment of WSON and amines by reducing ALWC, thereby effectively interrupting the self-amplifying cycle of SNA formation. These findings provide a new scientific basis for haze mitigation in high-humidity polluted regions.

**Data availability.**

The data including meteorological data, gaseous pollutants, and major chemical components in $PM_{2.5}$ are freely available from Gehui Wang.

**Supplement.**

The supplementary material is published as separate file with this article.

**Author contributions.**

GW designed the experiment and supervised the research. KC, RL, LC, RL, BX, SL and JZ collected the samples. KC, RL, LC, CW and GW conducted the sample analysis. KC, RL, LC, CW and GW performed the data interpretation. KC and GW

https://doi.org/10.5194/egusphere-2026-3616
Preprint. Discussion started: 10 July 2026


wrote the paper. ZL provided helpful assistance in writing the paper. All the authors contributed to the paper with useful scientific discussions.

**Competing interests.**

The contact author has declared that none of the authors has any competing interests.

**Disclaimer.**

Publisher's note: Copernicus Publications remains neutral with regard to jurisdictional claims made in the text, published maps, institutional affiliations, or any other geographical representation in this paper. While Copernicus Publications makes every effort to include appropriate place names, the final responsibility lies with the authors. Also, please note that this paper has not received English language copy-editing. Views expressed in the text are those of the authors and do not necessarily reflect the views of the publisher.

**Acknowledgements.**

This work was funded by the National Natural Science Foundation of China (grant nos. U23A2030, 42130704).

**Financial support.**

This research was financially supported by the National Natural Science Foundation of China (grant nos. U23A2030, 42130704).

**References**

Almeida, J., Schobesberger, S., Kürten, A., Ortega, I. K., Kupiainen-Määttä, O., Praplan, A. P., Adamov, A., Amorim, A., Bianchi, F., Breitenlechner, M., David, A., Dommen, J., Donahue, N. M., Downard, A., Dunne, E., Duplissy, J., Ehrhart, S., Flagan, R. C., Franchin, A., Guida, R., Hakala, J., Hansel, A., Heinritzi, M., Henschel, H., Jokinen, T., Junninen, H., Kajos, M., Kangasluoma, J., Keskinen, H., Kupc, A., Kurtén, T., Kvashin, A. N., Laaksonen, A., Lehtipalo, K., Leiminger, M., Leppä, J., Loukonen, V., Makhmutov, V., Mathot, S., McGrath, M. J., Nieminen, T., Olenius, T., Onnela, A., Petäjä, T., Riccobono, F., Riipinen, I., Rissanen, M., Rondo, L., Ruuskanen, T., Santos, F. D., Sarnela, N., Schallhart, S., Schnitzhofer, R., Seinfeld, J. H., Simon, M., Sipilä, M., Stozhkov, Y., Stratmann, F., Tomé, A., Tröstl, J., Tsagkogeorgas, G., Vaattovaara, P., Viisanen, Y., Virtanen, A., Vrtala, A., Wagner, P. E., Weingartner, E., Wex, H., Williamson, C., Wimmer, D., Ye, P., Yli-Juuti, T., Carslaw, K. S., Kulmala, M., Curtius, J., Baltensperger, U., Worsnop, D. R., Vehkamäki, H., and Kirkby, J.:

https://doi.org/10.5194/egusphere-2026-3616
Preprint. Discussion started: 10 July 2026


Molecular understanding of sulphuric acid–amine particle nucleation in the atmosphere, Nature, 502, 359-363, https://doi.org/10.1038/nature12663, 2013.

Brean, J., Bortolussi, F., Rowell, A., Beddows, D. C. S., Weinhold, K., Mettke, P., Merkel, M., Kumar, A., Barua, S., Iyer, S., Karppinen, A., Sandström, H., Rinke, P., Wiedensohler, A., Pöhlker, M., Dal Maso, M., Rissanen, M., Shi, Z., and Harrison, R. M.: Traffic-Emitted Amines Promote New Particle Formation at Roadsides, ACS ES&T Air, 2, 1704-1713, https://doi.org/10.1021/acsestair.5c00119, 2025.

Chen, Y., Xia, M., Zheng, P., Li, Y., Zou, Z., Tong, S., Li, K., Feng, X., Hui, L., Yuan, Q., Li, J., Yu, J. Z., Lee, S., Wang, T., and Wang, Z.: Complex gas-particle partitioning of nitro-phenolic compounds: field-based insights and determination of apparent activity coefficient, npj Clim. Atmos. Sci., 8, https://doi.org/10.1038/s41612-025-01156-z, 2025.

Chow, J. C., Watson, J. G., Chen, L. W. A., Chang, M. C. O., Robinson, N. F., Trimble, D., and Kohl, S.: The IMPROVE_A Temperature Protocol for Thermal/Optical Carbon Analysis: Maintaining Consistency with a Long-Term Database, J. Air Waste Manage. Assoc., 57, 1014-1023, https://doi.org/10.3155/1047-3289.57.9.1014, 2012.

Ditto, J. C., Abbatt, J. P. D., and Chan, A. W. H.: Gas- and Particle-Phase Amide Emissions from Cooking: Mechanisms and Air Quality Impacts, Environ. Sci. Technol., 56, 7741-7750, https://doi.org/10.1021/acs.est.2c01409, 2022.

Fountoukis, C., and Nenes, A.: ISORROPIA II: a computationally efficient thermodynamic equilibrium model for $K^+$ –$Ca^{2+}$ –$Mg^{2+}$ –$NH_4^+$ –$Na^+$ –$SO_4^{2-}$ –$NO_3^-$ –$Cl^-$ –$H_2O$ aerosols, Atmos. Chem. Phys., 7, 4639–4659, https://doi.org/10.5194/acp-7-4639-2007, 2007.

Ge, X., Wexler, A. S., and Clegg, S. L.: Atmospheric amines – Part II. Thermodynamic properties and gas/particle partitioning, Atmos. Environ., 45, 561-577, https://doi.org/10.1016/j.atmosenv.2010.10.013, 2011.

Gen, M., Huang, D. D., and Chan, C. K.: Reactive Uptake of Glyoxal by Ammonium-Containing Salt Particles as a Function of Relative Humidity, Environ. Sci. Technol., 52, 6903-6911, https://doi.org/10.1021/acs.est.8b00606, 2018.

Glasoe, W. A., Volz, K., Panta, B., Freshour, N., Bachman, R., Hanson, D. R., McMurry, P. H., and Jen, C.: Sulfuric acid nucleation: An experimental study of the effect of seven bases, J. Geophys. Res. Atmos., 120, 1933-1950, https://doi.org/10.1002/2014jd022730, 2015.

Guan, L., Ding, C., Zhang, Y., Hu, J., and Yu, X.: Pollution Characteristics and Sources of Water-soluble Organic Nitrogen in $PM_{2.5}$ in Jiangbei New Area，Nanjing, Environ. Sci., 43, 2888-2894, https://doi.org/10.13227/j.hjkx.202110026, 2022.

Guo, H., Xu, L., Bougiatioti, A., Cerully, K. M., Capps, S. L., Hite, J. R., Carlton, A. G., Lee, S. H., Bergin, M. H., Ng, N. L., Nenes, A., and Weber, R. J.: Fine-particle water and pH in the southeastern United States, Atmos. Chem. Phys., 15, 5211-5228, https://doi.org/10.5194/acp-15-5211-2015, 2015.

Hennigan, C. J., Izumi, J., Sullivan, A. P., Weber, R. J., and Nenes, A.: A critical evaluation of proxy methods used to estimate the acidity of atmospheric particles, Atmos. Chem. Phys., 15, 2775-2790, https://doi.org/10.5194/acp-15-2775-2015, 2015.

Jickells, T., Baker, A. R., Cape, J. N., Cornell, S. E., and Nemitz, E.: The cycling of organic nitrogen through the atmosphere, Philos. T. R. Soc. B, 368, https://doi.org/10.1098/rstb.2013.0115, 2013.

Kanawade, V. P., and Jokinen, T.: Atmospheric amines are a crucial yet missing link in Earth's climate via airborne aerosol production, Communications Earth & Environment, 6, https://doi.org/10.1038/s43247-025-02063-0, 2025.

Kürten, A., Jokinen, T., Simon, M., Sipilä, M., Sarnela, N., Junninen, H., Adamov, A., Almeida, J., Amorim, A., Bianchi, F., Breitenlechner, M., Dommen, J., Donahue, N. M., Duplissy, J., Ehrhart, S., Flagan, R. C., Franchin, A., Hakala, J., Hansel, A., Heinritzi, M., Hutterli, M., Kangasluoma, J., Kirkby, J., Laaksonen, A., Lehtipalo, K., Leiminger, M., Makhmutov, V., Mathot, S., Onnela, A., Petäjä, T., Praplan, A. P., Riccobono, F., Rissanen, M. P., Rondo, L., Schobesberger, S., Seinfeld, J. H., Steiner, G., Tomé, A., Tröstl, J., Winkler, P. M., Williamson, C., Wimmer, D., Ye, P., Baltensperger, U., Carslaw, K. S., Kulmala, M., Worsnop, D. R., and Curtius, J.: Neutral molecular cluster formation of sulfuric acid–dimethylamine observed in real time under atmospheric conditions, PNAS, 111, 15019-15024, https://doi.org/10.1073/pnas.1404853111, 2014.

https://doi.org/10.5194/egusphere-2026-3616
Preprint. Discussion started: 10 July 2026


Lehtipalo, K., Rondo, L., Kontkanen, J., Schobesberger, S., Jokinen, T., Sarnela, N., Kürten, A., Ehrhart, S., Franchin, A., Nieminen, T., Riccobono, F., Sipilä, M., Yli-Juuti, T., Duplissy, J., Adamov, A., Ahlm, L., Almeida, J., Amorim, A., Bianchi, F., Breitenlechner, M., Dommen, J., Downard, A. J., Dunne, E. M., Flagan, R. C., Guida, R., Hakala, J., Hansel, A., Jud, W., Kangasluoma, J., Kerminen, V.-M., Keskinen, H., Kim, J., Kirkby, J., Kupc, A., Kupiainen-Määttä, O., Laaksonen, A., Lawler, M. J., Leiminger, M., Mathot, S., Olenius, T., Ortega, I. K., Onnela, A., Petäjä, T., Praplan, A., Rissanen, M. P., Ruuskanen, T., Santos, F. D., Schallhart, S., Schnitzhofer, R., Simon, M., Smith, J. N., Tröstl, J., Tsagkogeorgas, G., Tomé, A., Vaattovaara, P., Vehkamäki, H., Vrtala, A. E., Wagner, P. E., Williamson, C., Wimmer, D., Winkler, P. M., Virtanen, A., Donahue, N. M., Carslaw, K. S., Baltensperger, U., Riipinen, I., Curtius, J., Worsnop, D. R., and Kulmala, M.: The effect of acid–base clustering and ions on the growth of atmospheric nano-particles, Nat. Commun., 7, https://doi.org/10.1038/ncomms11594, 2016.

Leung, C. W., Wang, X., and Hu, D.: Characteristics and source apportionment of water-soluble organic nitrogen (WSON) in $PM_{2.5}$ in Hong Kong: With focus on amines, urea, and nitroaromatic compounds, J. Hazard. Mater., 469, https://doi.org/10.1016/j.jhazmat.2024.133899, 2024.

Li, Z., Wang, G., Xiao, B., Li, R., Wu, C., Lv, S., Wu, F., Fu, Q., and Duan, Y.: Measurement report: simultaneous measurement on gas- and particle-phase water-soluble organics in Shanghai: enhanced light absorption of transported Asian dust, Atmos. Chem. Phys., 25, 12037-12049, https://doi.org/10.5194/acp-25-12037-2025, 2025.

Liu, F., Bi, X., Zhang, G., Lian, X., Fu, Y., Yang, Y., Lin, Q., Jiang, F., Wang, X., Peng, P. a., and Sheng, G.: Gas-to-particle partitioning of atmospheric amines observed at a mountain site in southern China, Atmos. Environ., 195, 1-11, https://doi.org/10.1016/j.atmosenv.2018.09.038, 2018.

Liu, X., Wang, H., Wang, F., Lv, S., Wu, C., Zhao, Y., Zhang, S., Liu, S., Xu, X., Lei, Y., and Wang, G.: Secondary Formation of Atmospheric Brown Carbon in China Haze: Implication for an Enhancing Role of Ammonia, Environ. Sci. Technol., 57, 11163-11172, https://doi.org/10.1021/acs.est.3c03948, 2023.

Lutz, A., Mohr, C., Le Breton, M., Lopez-Hilfiker, F. D., Priestley, M., Thornton, J. A., and Hallquist, M.: Gas to Particle Partitioning of Organic Acids in the Boreal Atmosphere, ACS Earth Space Chem., 3, 1279-1287, https://doi.org/10.1021/acsearthspacechem.9b00041, 2019.

Lv, S., Wang, F., Wu, C., Chen, Y., Liu, S., Zhang, S., Li, D., Du, W., Zhang, F., Wang, H., Huang, C., Fu, Q., Duan, Y., and Wang, G.: Gas-to-Aerosol Phase Partitioning of Atmospheric Water-Soluble Organic Compounds at a Rural Site in China: An Enhancing Effect of $NH_3$ on SOA Formation, Environ. Sci. Technol., 56, 3915-3924, https://doi.org/10.1021/acs.est.1c06855, 2022a.

Lv, S., Wu, C., Wang, F., Liu, X., Zhang, S., Chen, Y., Zhang, F., Yang, Y., Wang, H., Huang, C., Fu, Q., Duan, Y., and Wang, G.: Nitrate-Enhanced Gas-to-Particle-Phase Partitioning of Water-Soluble Organic Compounds in Chinese Urban Atmosphere: Implications for Secondary Organic Aerosol Formation, Environ. Sci. Technol. Lett., 10, 14-20, https://doi.org/10.1021/acs.estlett.2c00894, 2022b.

Matsumoto, K., Ogawa, T., Ishikawa, M., Hirai, A., Watanabe, Y., and Nakano, T.: Organic and inorganic nitrogen deposition on the red pine forests at the northern foot of Mt. Fuji, Japan, Atmos. Environ., 237, https://doi.org/10.1016/j.atmosenv.2020.117676, 2020.

Mochizuki, T., Kawamura, K., and Aoki, K.: Water-Soluble Organic Nitrogen in High Mountain Snow Samples from Central Japan, Aerosol Air Qual. Res., 16, 632-639, https://doi.org/10.4209/aaqr.2015.04.0256, 2016.

Murray, D. S., Shattuck, M. D., McDowell, W. H., and Wymore, A. S.: Nitrogen wet deposition stoichiometry: the role of organic nitrogen, seasonality, and snow, Biogeochemistry, 160, 301-314, https://doi.org/10.1007/s10533-022-00966-0, 2022.

Nehir, M., and Koçak, M.: Atmospheric water-soluble organic nitrogen (WSON) in the eastern Mediterranean: origin and ramifications regarding marine productivity, Atmos. Chem. Phys., 18, 3603-3618, https://doi.org/10.5194/acp-18-3603-2018, 2018.

Nursanto, F. R., He, Q., van de Wouw, S., Zanders, A., Hohaus, T., Kroese, W. S. J., Wegener, R., Adam, M. G., Winter, B., Dubus, R., Kesper, L., Rohrer, F., Wang, Y., Matthews, E., Voliotis,

https://doi.org/10.5194/egusphere-2026-3616
Preprint. Discussion started: 10 July 2026


A., Bannan, T. J., McFiggans, G., Coe, H., Wu, Y., Roska, M., Canagaratna, M., Alton, M., Coggon, M. M., Stockwell, C. E., Bates, K. H., Pfannerstill, E. Y., Zorn, S. R., Wang, H., Riva, M., Perrier, S., Yang, B., Liu, L., Novelli, A., Färber, M., Fuchs, H., Marcillo Lara, A. C., Grasse, A., Wesolek, C., Tillmann, R., Holzinger, R., Krol, M. C., Gkatzelis, G. I., and Fry, J. L.: Gas-particle partitioning, molecular weight, and yield of organic nitrate under different urban VOC, $NO_x$, and oxidation conditions during SAPHIR-CHANEL campaign, EGUsphere, 2026, 1-38, https://doi.org/10.5194/egusphere-2025-6310, 2026.

Özel, M. Z., Ward, M. W., Hamilton, J. F., Lewis, A. C., Raventós-Duran, T., and Harrison, R. M.: Analysis of Organic Nitrogen Compounds in Urban Aerosol Samples Using GCxGC-TOF/MS, Aerosol Science and Technology, 44, 109-116, https://doi.org/10.1080/02786820903410105, 2010.

Pankow, J. F.: An absorption model of gas/particle partitioning of organic compounds in the atmosphere, Atmos. Environ., 28, 185-188, https://doi.org/10.1016/1352-2310(94)90093-0, 1994.

Pankow, J. F.: Phase considerations in the gas/particle partitioning of organic amines in the atmosphere, Atmos. Environ., 122, 448-453, https://doi.org/10.1016/j.atmosenv.2015.09.056, 2015.

Pleim, J., and Ran, L.: Surface Flux Modeling for Air Quality Applications, Atmosphere, 2, 271-302, https://doi.org/10.3390/atmos2030271, 2011.

Qiu, C., and Zhang, R.: Multiphase chemistry of atmospheric amines, Physical Chemistry Chemical Physics, 15, https://doi.org/10.1039/c3cp43446j, 2013.

Rollins, A. W., Smith, J. D., Wilson, K. R., and Cohen, R. C.: Real Time In Situ Detection of Organic Nitrates in Atmospheric Aerosols, Environ. Sci. Technol., 44, 5540-5545, https://doi.org/10.1021/es100926x, 2010.

Sareen, N., Waxman, E. M., Turpin, B. J., Volkamer, R., and Carlton, A. G.: Potential of Aerosol Liquid Water to Facilitate Organic Aerosol Formation: Assessing Knowledge Gaps about Precursors and Partitioning, Environ. Sci. Technol., 51, 3327-3335, https://doi.org/10.1021/acs.est.6b04540, 2017.

Schobesberger, S., Junninen, H., Bianchi, F., Lönn, G., Ehn, M., Lehtipalo, K., Dommen, J., Ehrhart, S., Ortega, I. K., Franchin, A., Nieminen, T., Riccobono, F., Hutterli, M., Duplissy, J., Almeida, J., Amorim, A., Breitenlechner, M., Downard, A. J., Dunne, E. M., Flagan, R. C., Kajos, M., Keskinen, H., Kirkby, J., Kupc, A., Kürten, A., Kurtén, T., Laaksonen, A., Mathot, S., Onnela, A., Praplan, A. P., Rondo, L., Santos, F. D., Schallhart, S., Schnitzhofer, R., Sipilä, M., Tomé, A., Tsagkogeorgas, G., Vehkamäki, H., Wimmer, D., Baltensperger, U., Carslaw, K. S., Curtius, J., Hansel, A., Petäjä, T., Kulmala, M., Donahue, N. M., and Worsnop, D. R.: Molecular understanding of atmospheric particle formation from sulfuric acid and large oxidized organic molecules, PNAS, 110, 17223-17228, https://doi.org/10.1073/pnas.1306973110, 2013.

Silvern, R. F., Jacob, D. J., Kim, P. S., Marais, E. A., Turner, J. R., Campuzano-Jost, P., and Jimenez, J. L.: Inconsistency of ammonium–sulfate aerosol ratios with thermodynamic models in the eastern US: a possible role of organic aerosol, Atmos. Chem. Phys., 17, 5107-5118, https://doi.org/10.5194/acp-17-5107-2017, 2017.

Stangl, C. M., and Johnston, M. V.: Aqueous Reaction of Dicarbonyls with Ammonia as a Potential Source of Organic Nitrogen in Airborne Nanoparticles, J. Phys. Chem. A, 121, 3720-3727, https://doi.org/10.1021/acs.jpca.7b02464, 2017.

Tang, S., Li, F., Lv, J., Liu, L., Wu, G., Wang, Y., Yu, W., Wang, Y., and Jiang, G.: Unexpected molecular diversity of brown carbon formed by Maillard-like reactions in aqueous aerosols, Chemical Science, 13, 8401-8411, https://doi.org/10.1039/d2sc02857c, 2022.

Tao, Y., Ye, X., Jiang, S., Yang, X., Chen, J., Xie, Y., and Wang, R.: Effects of amines on particle growth observed in new particle formation events, J. Geophys. Res. Atmos., 121, 324-335, https://doi.org/10.1002/2015jd024245, 2016.

Tilgner, A., Schaefer, T., Alexander, B., Barth, M., Collett Jr, J. L., Fahey, K. M., Nenes, A., Pye, H. O. T., Herrmann, H., and McNeill, V. F.: Acidity and the multiphase chemistry of atmospheric aqueous particles and clouds, Atmos. Chem. Phys., 21, 13483-13536, https://doi.org/10.5194/acp-21-13483-2021, 2021.

https://doi.org/10.5194/egusphere-2026-3616
Preprint. Discussion started: 10 July 2026


Vione, D., Maurino, V., Minero, C., Lucchiari, M., and Pelizzetti, E.: Nitration and hydroxylation of benzene in the presence of nitrite/nitrous acid in aqueous solution, Chemosphere, 56, 1049-1059, https://doi.org/10.1016/j.chemosphere.2004.05.027, 2004.

Wang, S., Shao, P., Yang, X., Wu, J., Zhang, S., Zeng, S., Fan, J., Ni, C., and Wang, S.: Impact of photochemistry on wintertime haze in the Southern Sichuan Basin, China, Atmos. Pollut. Res., 15, https://doi.org/10.1016/j.apr.2024.102300, 2024.

Wang, Y., Hu, M., Wang, Y., Zheng, J., Shang, D., Yang, Y., Liu, Y., Li, X., Tang, R., Zhu, W., Du, Z., Wu, Y., Guo, S., Wu, Z., Lou, S., Hallquist, M., and Yu, J. Z.: The formation of nitro-aromatic compounds under high NO<sub><i>x</i></sub> and anthropogenic VOC conditions in urban Beijing, China, Atmos. Chem. Phys., 19, 7649-7665, https://doi.org/10.5194/acp-19-7649-2019, 2019.

Xiao, B., Wang, G., Li, Z., Li, R., Liang, C., Wang, H., Zhang, S., Wu, C., Li, R., Zhang, F., Zhang, R., Wu, Y., and Zhang, L.: High Contribution of Secondary Formation to Brown Carbon in China Humid Haze: Enhancing Role of Ammonia and Amines, Environ. Sci. Technol., 59, 27530-27540, https://doi.org/10.1021/acs.est.5c13436, 2025.

Xie, F., Wang, F., Li, L., Peng, C., Zhou, X., Sun, Y., and Lü, C.: Characteristics and sources of water-soluble organic nitrogen in $PM_{2.5}$ from a resource-dependent city, Atmos. Pollut. Res., 16, https://doi.org/10.1016/j.apr.2025.102586, 2025.

Xu, X., Wang, G., Gao, Y., Zhang, S., Chen, L., Li, R., Li, Z., and Li, R.: Smog chamber study on the $NO_x$ dependence of SOA from isoprene photo-oxidation: Implication on $RO_2$ chemistry, J. Environ. Sci., 161, 752-760, https://doi.org/10.1016/j.jes.2025.05.024, 2026.

Xu, Y., Miyazaki, Y., Tachibana, E., Sato, K., Ramasamy, S., Mochizuki, T., Sadanaga, Y., Nakashima, Y., Sakamoto, Y., Matsuda, K., and Kajii, Y.: Aerosol Liquid Water Promotes the Formation of Water-Soluble Organic Nitrogen in Submicrometer Aerosols in a Suburban Forest, Environ. Sci. Technol., 54, 1406-1414, https://doi.org/10.1021/acs.est.9b05849, 2020.

Yang, D., Zhu, S., Ma, Y., Zhou, L., Zheng, F., Wang, L., Jiang, J., and Zheng, J.: Emissions of Ammonia and Other Nitrogen-Containing Volatile Organic Compounds from Motor Vehicles under Low-Speed Driving Conditions, Environ. Sci. Technol., 56, 5440-5447, https://doi.org/10.1021/acs.est.2c00555, 2022.

Yang, X., Cao, F., Fan, M., Lin, Y., Xie, F., and Zhang, Y.: Seasonal variations of low molecular alkyl amines in $PM_{2.5}$ in a North China Plain industrial city: Importance of secondary formation and combustion emissions, Sci. Total Environ., 857, https://doi.org/10.1016/j.scitotenv.2022.159371, 2023.

Yao, L., Garmash, O., Bianchi, F., Zheng, J., Yan, C., Kontkanen, J., Junninen, H., Mazon, S. B., Ehn, M., Paasonen, P., Sipilä, M., Wang, M. Y., Wang, X. K., Xiao, S., Chen, H. F., Lu, Y. Q., Zhang, B. W., Wang, D. F., Fu, Q. Y., Geng, F. H., Li, L., Wang, H. L., Qiao, L. P., Yang, X., Chen, J. M., Kerminen, V. M., Petäjä, T., Worsnop, D. R., Kulmala, M., and Wang, L.: Atmospheric new particle formation from sulfuric acid and amines in a Chinese megacity, Science, 361, 278-+, https://doi.org/10.1126/science.aao4839, 2018.

Yu, H., McGraw, R., and Lee, S. H.: Effects of amines on formation of sub-3 nm particles and their subsequent growth, Geophys. Res. Lett., 39, https://doi.org/10.1029/2011gl050099, 2012.

Yu, Q., Fu, N., Lu, J., Zhang, Y., Du, W., and Wang, J.: Atmospheric Amines: Advances in Analytical Techniques, Emission Inventories, Regional Pollution, and Roles in New Particle Formation, Current Pollution Reports, 11, https://doi.org/10.1007/s40726-025-00364-8, 2025.

Yu, X., Yu, Q., Zhu, M., Tang, M., Li, S., Yang, W., Zhang, Y., Deng, W., Li, G., Yu, Y., Huang, Z., Song, W., Ding, X., Hu, Q., Li, J., Bi, X., and Wang, X.: Water Soluble Organic Nitrogen (WSON) in Ambient Fine Particles Over a Megacity in South China: Spatiotemporal Variations and Source Apportionment, J. Geophys. Res. Atmos., 122, https://doi.org/10.1002/2017jd027327, 2017.

Yu, X., Li, D., Li, D., Zhang, G., Zhou, H., Li, S., Song, W., Zhang, Y., Bi, X., Yu, J., and Wang, X.: Enhanced Wet Deposition of Water-Soluble Organic Nitrogen During the Harvest Season: Influence of Biomass Burning and In-Cloud Scavenging, J. Geophys. Res. Atmos., 125, https://doi.org/10.1029/2020jd032699, 2020.

https://doi.org/10.5194/egusphere-2026-3616
Preprint. Discussion started: 10 July 2026


662 Yu, X., Li, Q., Liao, K., Li, Y., Wang, X., Zhou, Y., Liang, Y., and Yu, J. Z.: New measurements
663 reveal a large contribution of nitrogenous molecules to ambient organic aerosol, npj Clim.
664 Atmos. Sci., 7, https://doi.org/10.1038/s41612-024-00620-6, 2024.
665 Yuan, B., Liggio, J., Wentzell, J., Li, S.-M., Stark, H., Roberts, J. M., Gilman, J., Lerner, B.,
666 Warneke, C., Li, R., Leithead, A., Osthoff, H. D., Wild, R., Brown, S. S., and de Gouw, J. A.:
667 Secondary formation of nitrated phenols: insights from observations during the Uintah Basin
668 Winter Ozone Study (UBWOS) 2014, Atmos. Chem. Phys., 16, 2139-2153,
669 https://doi.org/10.5194/acp-16-2139-2016, 2016.
670 Zhang, J., Li, J., Su, Y., Chen, C., Chen, L., Huang, X., Wang, F., Huang, Y., and Wang, G.:
671 Interannual evolution of the chemical composition, sources and processes of $PM_{2.5}$ in
672 Chengdu, China: Insights from observations in four winters, J. Environ. Sci., 138, 32-45,
673 https://doi.org/10.1016/j.jes.2023.02.055, 2024a.
674 Zhang, J., Su, Y., Chen, C., Guo, W., Tan, Q., Feng, M., Song, D., Jiang, T., Chen, Q., Li, Y., Li,
675 W., Wang, Y., Huang, X., Han, L., Wu, W., and Wang, G.: Chemical composition, sources
676 and formation mechanism of urban $PM_{2.5}$ in Southwest China: a case study at the beginning
677 of 2023, Atmos. Chem. Phys., 24, 2803-2820, https://doi.org/10.5194/acp-24-2803-2024,
678 2024b.
679 Zhang, S., Wang, G., Xu, X., Liu, Y., Nie, W., Chen, L., Li, R., Gao, Y., Li, R., Wu, C., Zhang, J.,
680 and Prevot, A. S. H.: Unappreciated Role of Photochemical Aging of Biogenic Organic
681 Nitrates in Atmospheric Ozone Formation, Environ. Sci. Technol.,
682 https://doi.org/10.1021/acs.est.5c11688, 2026.
683 Zhu, S., Yan, C., Zheng, J., Chen, C., Ning, H., Yang, D., Wang, M., Ma, Y., Zhan, J., Hua, C., Yin,
684 R., Li, Y., Liu, Y., Jiang, J., Yao, L., Wang, L., Kulmala, M., and Worsnop, D. R.: Observation
685 and Source Apportionment of Atmospheric Alkaline Gases in Urban Beijing, Environ. Sci.
686 Technol., 56, 17545-17555, https://doi.org/10.1021/acs.est.2c03584, 2022.
687

https://doi.org/10.5194/egusphere-2026-3616
Preprint. Discussion started: 10 July 2026


688 **Table 1.** Concentrations of major pollutants and meteorological parameters in
689 Sichuan Basin (SCB), China during winter (μg $m^{-3}$).

| Specie | Whole | Clean Period | Transition Period | Pollution Period |
|---|---|---|---|---|
| I. Gas pollutants | | | | |
| $NH_3$ | 12.3 ± 3.6 (2.4–31.2) | 8.1 ± 2.7 (2.9–11.5) | 11.8 ± 3.5 (3.4–31.2) | 13.5 ± 3.0 (5.1–21.6) |
| $WSON_g$[a] | 1.2 ± 0.9 (0.1–5.8) | 0.7 ± 0.5 (0.1–1.7) | 1.0 ± 0.7 (0.1–3.9) | 1.4 ± 1.1 (0.1–5.8) |
| $WSOC_g$[b] | 22.6 ± 9.8 (4.4–69.8) | 16.6 ± 7.9 (4.4–31.3) | 20.3 ± 8.8 (4.8–51.5) | 25.5 ± 9.8 (6.2–69.8) |
| $CH_3NH_2$ | 1.23 ± 0.36 (0.46–2.90) | 0.84 ± 0.21 (0.46–1.26) | 1.19 ± 0.37 (0.46–2.90) | 1.35 ± 0.32 (0.59–2.32) |
| $(CH_3)_2NH$ | 0.41 ± 0.03 (0.34–0.68) | 0.38 ± 0.02 (0.34–0.42) | 0.40 ± 0.03 (0.34–0.68) | 0.42 ± 0.03 (0.35–0.53) |
| II. Major components of $PM_{2.5}$ | | | | |
| $PM_{2.5}$ | 76 ± 38 (7–199) | 29 ± 11 (7–49) | 55 ± 18 (9–101) | 100 ± 33 (30–199) |
| $SO_4^{2-}$ | 4.9 ± 2.0 (1.5–11.9) | 2.9 ± 1.2 (1.5–6.0) | 3.7 ± 1.0 (1.6–6.7) | 6.2 ± 1.7 (2.9–11.9) |
| $NO_3^-$ | 16.7 ± 8.3 (2.9–39.0) | 6.4 ± 32.1 (2.9–11.0) | 12.0 ± 4.0 (3.4–22.3) | 22.3 ± 7.2 (6.4–39.0) |
| $Cl^-$ | 1.3 ± 1.0 (0.1–6.1) | 0.5 ± 0.2 (0.1–0.9) | 1.0 ± 0.7 (0.1–6.0) | 1.8 ± 1.1 (0.3–6.1) |
| $NH_4^+$ | 7.2 ± 3.0 (1.4–15.5) | 3.5 ± 0.8 (2.1–5.5) | 5.6 ± 1.7 (1.4–10.3) | 9.1 ± 2.6 (3.0–15.5) |
| Other ions[c] | 2.2 ± 1.1 (0.8–9.1) | 1.2 ± 0.2 (0.8–1.9) | 1.7 ± 0.5 (0.9–3.5) | 2.8 ± 1.2 (1.1–9.1) |
| OM[d] | 21.1 ± 9.6 (6.7–47.4) | 9.5 ± 1.9 (6.7–11.3) | 15.1 ± 3.5 (6.9–21.0) | 25.6 ± 9.3 (8.1–47.4) |
| $WSON_p$[a] | 2.3 ± 1.4 (0.1–6.3) | 1.0 ± 0.9 (0.1－4.3) | 1.5 ± 0.8 (0.1－4.9) | 3.0 ± 1.4 (0.3－6.3) |
| $WSOC_p$[b] | 13.5 ± 7.2 (1.2–56.2) | 8.1 ± 4.5 (1.4–21.0) | 10.9 ± 6.6 (1.2–56.2) | 16.3 ± 6.8 (2.7–54.8) |
| $CH_3NH_3^+$ | 0.45 ± 0.24 (0.03–1.27) | 0.18 ± 0.06 (0.10–0.34) | 0.33 ± 0.13 (0.03–0.67) | 0.61 ± 0.23 (0.15–1.27) |
| $(CH_3)_2NH_2^+$ | 0.09 ± 0.05 (0.02–0.34) | 0.06 ± 0.01 (0.04–0.09) | 0.07 ± 0.04 (0.02–0.29) | 0.12 ± 0.04 (0.05–0.34) |
| III. Gas-particle partitioning coefficients of WSON, WSOC, MA, DMA | | | | |
| $F_{WSON}$[e] | 0.70 ± 0.14 (0.28–0.98) | 0.62 ± 0.17 (0.29–0.88) | 0.66 ± 0.14 (0.28–0.90) | 0.73 ± 0.13 (0.42–0.98) |
| $F_{WSOC}$[e] | 0.36 ± 0.09 (0.10–0.81) | 0.32 ± 0.10 (0.19–0.65) | 0.34 ± 0.09 (0.13–0.75) | 0.39 ± 0.09 (0.10–0.81) |
| $F_{MA}$[e] | 0.25 ± 0.08 (0.07–0.44) | 0.18 ± 0.06 (0.09–0.31) | 0.21 ± 0.06 (0.07–0.39) | 0.30 ± 0.06 (0.12–0.40) |
| $F_{DMA}$[e] | 0.18 ± 0.06 (0.04–0.45) | 0.13 ± 0.02 (0.10–0.19) | 0.15 ± 0.06 (0.04–0.42) | 0.21 ± 0.05 (0.12–0.45) |
| IV. Meteorology parameters and aerosol properties | | | | |
| T (°C) | 6.4 ± 3.6 (-2.4–16.5) | 6.2 ± 2.7 (0.2–12.3) | 6.4 ± 3.4 (-1.3–15.4) | 6.4 ± 3.9 (-2.4–16.5) |
| RH (%) | 78 ± 19 (20–100) | 78 ± 22 (26–99) | 76 ± 19 (20–100) | 79 ± 18 (29–100) |
| WS (m/s) | 0.5 ± 0.4 (0.0–1.7) | 0.6 ± 0.3 (0.0–1.4) | 0.6 ± 0.4 (0.0–1.7) | 0.3 ± 0.3 (0.0–0.9) |
| pH of $PM_{2.5}$ | 4.4 ± 0.2 (3.4–5.0) | 4.2 ± 0.3 (3.4–4.5) | 4.4 ± 0.2 (3.6–4.9) | 4.4 ± 0.2 (3.8–5.0) |
| ALWC[f] | 64.0 ± 71.5 (0.5–422.2) | 34.0 ± 35.8 (1.2–130.5) | 44.4 ± 49.2 (0.5–215.9) | 87.6 ± 85.1 (1.6–422.2) |

690 [a] $WSON_g$ is the gas-phase organics, $WSON_p$ is the organics in $PM_{2.5}$, (μgN $m^{-3}$). [b]
691 $WSOC_g$ is the gas-phase organics, $WSOC_p$ is the organics in $PM_{2.5}$, (μgC $m^{-3}$). [c] Other
692 ions are the sum of $NO_2^-$, $F^-$, $K^+$, $Na^+$, $Mg^{2+}$, and $Ca^{2+}$. [d] Organic matter: OM = OC ×
693 1.6. [e] $F_p = C_p/(C_g+C_p)$. [f] ALWC: aerosol liquid water content of $PM_{2.5}$.

694

https://doi.org/10.5194/egusphere-2026-3616
Preprint. Discussion started: 10 July 2026


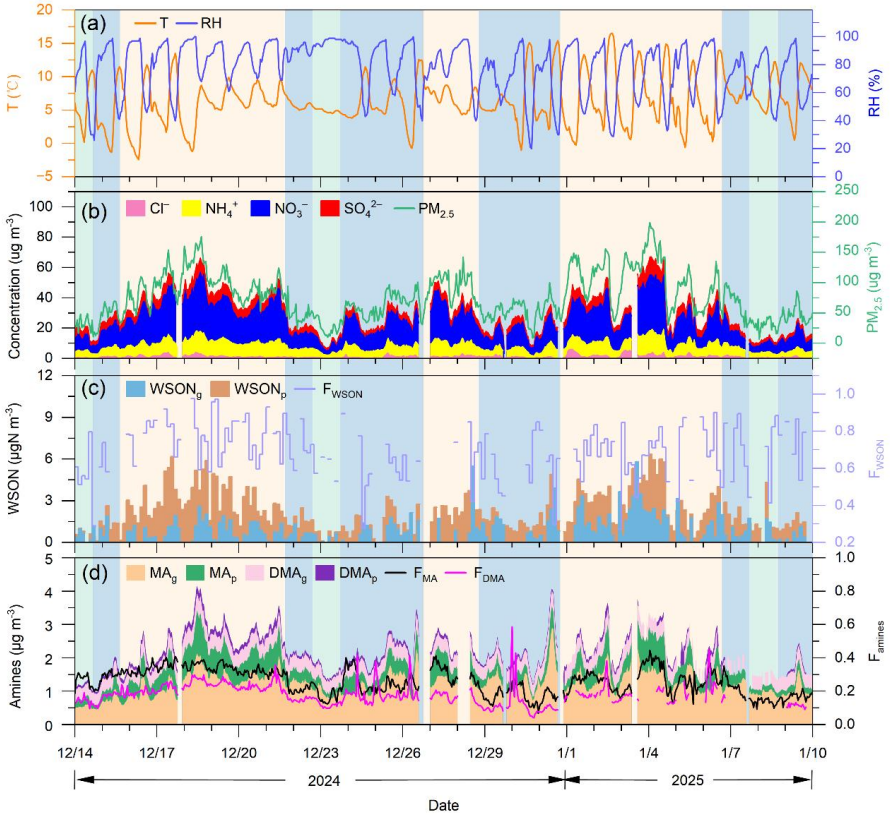


**Figure 1.** Temporal variation of major pollutants in Chengdu, China, during the winter of 2024 – 2025. $F_p$ =$C_p$/($C_g$+$C_p$), $C_p$ and $C_g$ are the concentrations of WSON and methylamine (MA) or dimethylamine (DMA) in the particle phase and gas phase, respectively. Green shadows represent clean periods with $PM_{2.5} \in [0, 35)$ μg m$^{-3}$. Blue shadows represent transition periods with $PM_{2.5} \in [35, 75)$ μg m$^{-3}$. Orange shadows represent pollution periods with $PM_{2.5} \in [75, 200)$ μg m$^{-3}$.

https://doi.org/10.5194/egusphere-2026-3616
Preprint. Discussion started: 10 July 2026


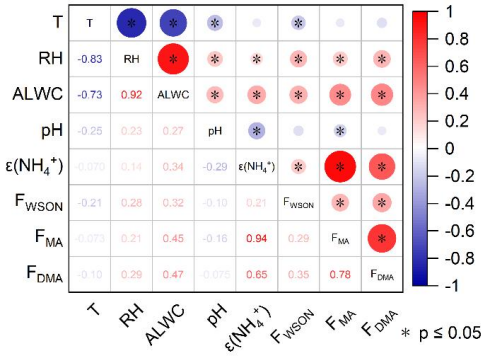


**Figure 2.** Factors affecting the gas-to-aerosol phase partitioning coefficients of WSON ($F_{WSON}$), methylamine ($F_{MA}$) and dimethylamine ($F_{DMA}$) in the SCB region of China.

https://doi.org/10.5194/egusphere-2026-3616
Preprint. Discussion started: 10 July 2026


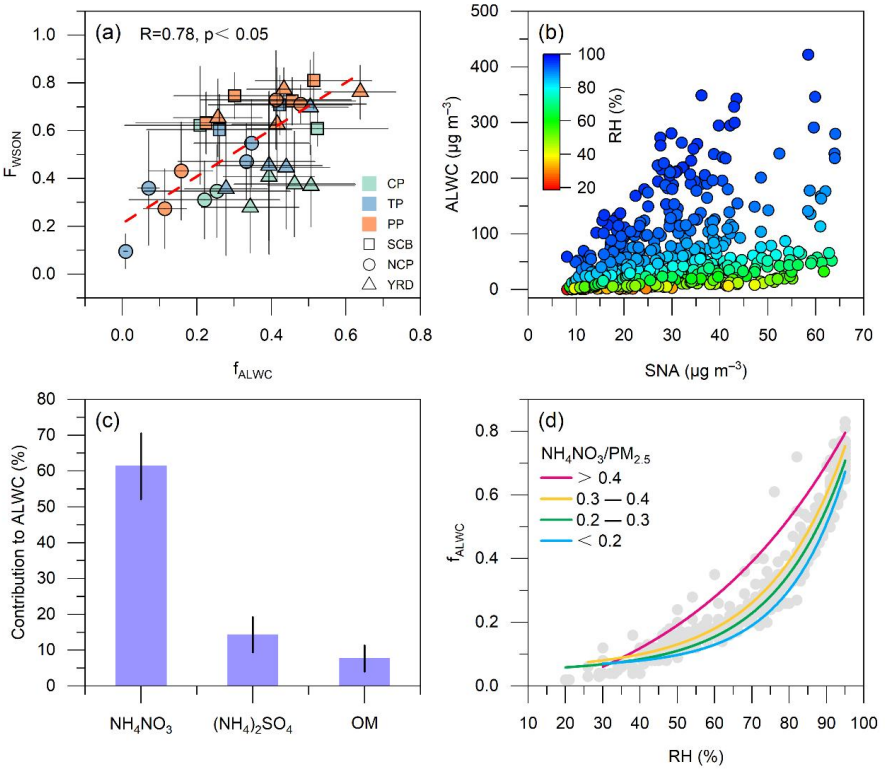


**Figure 3.** Chemical drivers of ALWC and its associations with WSON. (a) correlation between the relative abundance of ALWC to $PM_{2.5}$ ($f_{ALWC}$= ALWC/(ALWC+$PM_{2.5}$)) and $F_{WSON}$. Symbols represent different geographical regions (YRD: Yangtze River Delta; NCP: North China Plain; SCB: Sichuan Basin), colors denote different pollution periods (PP: polluted period; TP: transition period; CP: clean period). (b) relationship between ALWC and SNA concentrations during the whole campaign of SCB, colored by RH. (c) mean percentage contribution (± 1 SD) of different chemical components ($NH_4NO_3$, $(NH_4)_2SO_4$, OM) to ALWC during the whole campaign of SCB. (d) variation of $f_{ALWC}$ with RH under different relative abundances of $NH_4NO_3$ to $PM_{2.5}$ during the whole campaign in the SCB (solid lines represent the fitted curves, and gray dots represent the raw data).

https://doi.org/10.5194/egusphere-2026-3616
Preprint. Discussion started: 10 July 2026


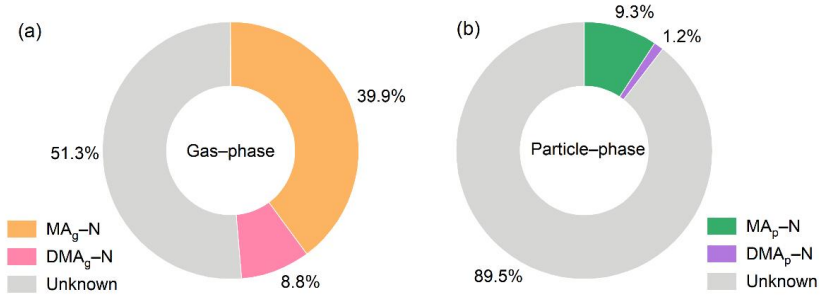


**Figure 4.** Contributions of amines N concentrations to gas-phase (a) and particulate-phase (b) WSON.

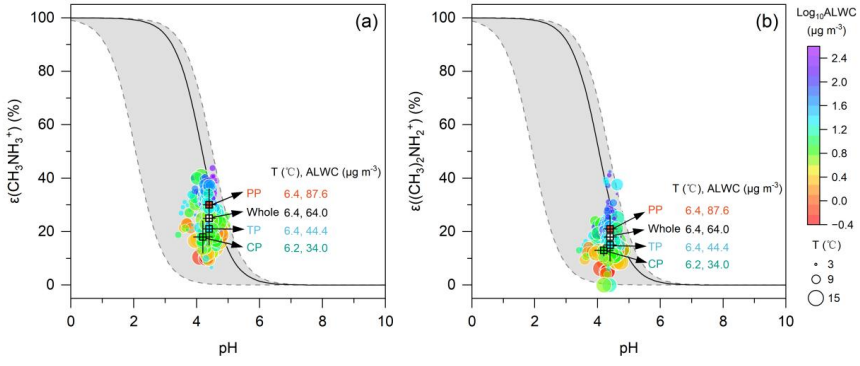


**Figure 5.** Analytically calculated S-curves of $\varepsilon(CH_3NH_3^+)$ and $\varepsilon((CH_3)_2NH_2^+)$ and ambient data during the entire observation period. Circles represent the measured data for methylamine (a) and dimethylamine (b), respectively. For the analytically calculated S-curve, we used $\gamma_{CH_3NH_3^+} = \gamma_{(CH_3)_2NH_2^+} = 0.338$, $\gamma_{CH_3NH_2} = \gamma_{(CH_3)_2NH} = 1.240$, and $\gamma_{H^+} = 0.836$ (E-AIM model predicted). The black solid line is the S-curve calculated based on the average temperature and ALWC (6.4 ± 3.6 ℃ and 63.99 ± 71.53 μg m$^{-3}$, respectively). The gray dashed line represents the S-curve calculated using 1 standard deviation of the average temperature and ALWC. Due to the value of ALWC minus 1 standard deviation being less than 0, the minimum ALWC value (i.e., $W_i$ = 0.48 μg m$^{-3}$) was used in the calculation. Different colors and blocks represent different sampling periods and their corresponding average values. CP: clean period, TP: transition period, PP: pollution period, and Whole: whole campaign period.